Experimental Demonstration of an 8-Gbit/s QPSK Coherent Underwater Wireless Optical Communication Link Under Scattering Conditions

Yuxiang Duan[1*], Huibin Zhou[1], Zile Jiang[1], Muralekrishnan Ramakrishnan[1], Xinzhou Su[1], Wing Ko[1], Yue Zuo[1], Hongkun Lian[1], Zixun Zhao[1], Ruoyu Zeng[1], Yingning Wang[1], Moshe Tur[2], and Alan E. Willner[1,3]

*1. Dept. of Electrical Engineering, University of Southern California, Los Angeles, CA 90089, USA, *yuxiangd@usc.edu*

2. School of Electrical Engineering, Tel Aviv University, Ramat Aviv 69978, ISRAEL

3. Dornsife Dept. of Physics & Astronomy, University of Southern California, Los Angeles, CA 90089, USA

Abstract: We experimentally demonstrate an 8-Gbit/s QPSK coherent underwater wireless optical communication link under scattering conditions at 532 nm. We achieve BER below 20% FEC limit under attenuation length up to 6.5, and the corresponding receiver sensitivity is -29.8 dBm.

1. Introduction

As compared to acoustic-wave communications, there is growing interest in optics for underwater communication links to achieve relatively high bit rates over many meters [1,2]. Given the extremely high absorption of radio waves and infrared light in water, the spectrum of choice for underwater seems to be in the blue-green region [3,4]. Importantly, underwater conditions may be fairly harsh in that a highly turbid underwater medium can induce significant degradations (e.g., high loss due to scattering) [4,5].

To date, the majority of reported underwater links tend to involve direct detection of amplitude-encoded data channels [6-9]. However, as is the case for most optical communication systems, there is a benefit to using coherent detection in order to enable: (i) the recovery of phase-encoded data channels of higher-order modulation formats (e.g., quadrature-phase-shift-keyed (QPSK) and quadrature-amplitude-modulation (QAM)), (ii) higher sensitivity when using a relatively high-power local oscillator (LO) in the receiver (Rx), and (iii) the use of electronic digital signal processing (DSP) to mitigate channel degradations [10].

Previous reports of underwater links of phase-encoded data channels with scattering include: (a) direct detection links (without LO) using multi-carrier modulations, e.g. orthogonal frequency-division multiplexing (OFDM), discrete multitone (DMT) [11-15], and (b) coherent link of 8-PSK 0.5-Gbaud data, where, however, the same laser is split and used at the transmitter (Tx) for the data and at the Rx for the LO [16]. A laudable goal might be to enable a coherent underwater link that uses an independent LO at the Rx.

In this paper, we experimentally demonstrate an 8-Gbit/s QPSK coherent underwater wireless optical communication (UWOC) link under scattering conditions. We first modulate a 1064-nm laser with a phase modulator and then convert it to 532 nm using the second harmonic generation (SHG) through a periodically poled $LiNbO_3$ (PPLN). The 1064-nm signal with 4 phase levels of an 8-PSK format is phase doubled to generate a 532-nm QPSK signal during SHG at the Tx [17]. We transmit the QPSK data channel through a 0.6-meter water tank with emulated scattering effects. At the Rx, the LO at ~532 nm is generated by converting a separate ~1064-nm laser using another PPLN. The received QPSK data beam is mixed with the independent LO for coherent heterodyne detection. Our results show that the bit-error rates (BERs) of the detected QPSK signal can reach below the 20% soft-decision forward error correction (SD-FEC) limit under turbid water with attenuation length (γL) up to 8.2 and 6.5 for 2- and 8-Gbit/s QPSK, respectively, which may potentially support distance of up to 20 m over coastal ocean (γ = ~0.4 m^{-1}) [4]. The corresponding receiver sensitivity achieved in our experiment is -37.8 dBm and -29.8 dBm for 2- and 8-Gbit/s QPSK, respectively.

2. Concept and experimental setup

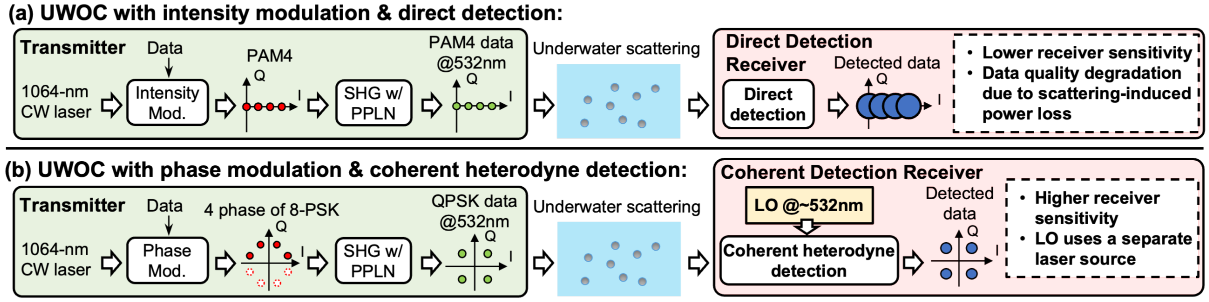

Fig. 1 (a) Concept of UWOC through scattering using intensity modulation & direct detection. (b) Concept of coherent UWOC utilizing phase modulation & coherent heterodyne detection. A separate laser is used as the local oscillator (LO) to enhance the receiver sensitivity.

Figure 1 (a) shows the concept of UWOC through scattering with intensity modulation & direct detection (IM/DD). At the Tx, the high-speed intensity-modulated signal (e.g., four-level pulse amplitude modulation (PAM4)) at 532 nm is generated by an external intensity modulator at 1064 nm followed by SHG through PPLN crystal. However, due to the underwater scattering effect, optical power reaching the Rx may be close or lower to its sensitivity, resulting in a significantly degraded data quality. Fig. 1 (b) shows the concept of using phase modulation & coherent heterodyne detection to increase the receiver sensitivity of UWOC. At the Tx, the 1064-nm CW laser is modulated with the first 4 phase levels of an 8-PSK format by a phase modulator. After the SHG, QPSK data at 532 nm is generated due to the phase doubling process through PPLN [17]. At the Rx, the received data beam is combined and mixed with a relatively high-power LO at 532 nm from a separate laser source for coherent detection. Compared to IM/DD, the coherent detection scheme has a higher receiver sensitivity and can provide better signal quality through scattering due to the use of the local oscillator. Although this paper demonstrates a QPSK coherent link, we believe our approach can also support higher-order complex modulation formats (e.g., 16-QAM) by using an I /Q modulator at 1064 nm.

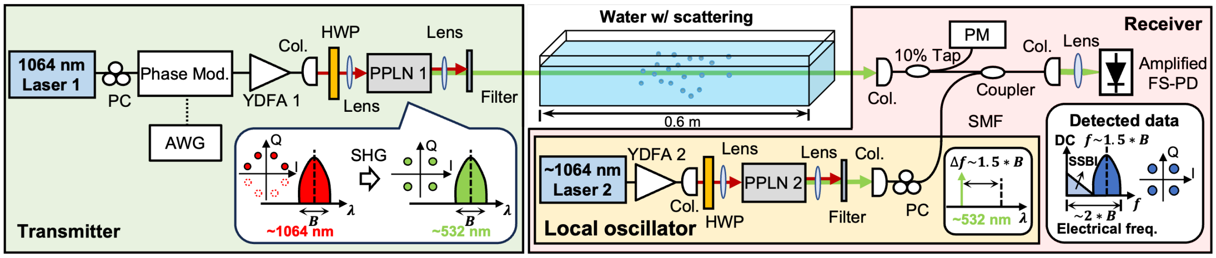

Fig. 2. Experimental setup of the coherent UWOC link through underwater scattering. AWG: arbitrary waveform generator; Col.: collimator; HWP: half-wave plate; LO: local oscillator; PC: polarization controller; PM: power meter; PPLN: periodically poled lithium niobate; SMF: single-mode fiber; YDFA: ytterbium-doped fiber amplifier; FS-PD: free-space coupled photodiode.

Figure 2 represents the experimental setup. At the Tx, a CW laser at 1064 nm is modulated by a phase modulator, amplified by a YDFA, and converted to a 532-nm light beam by SHG through PPLN. During the SHG, the phase of the 1064-nm signal is doubled, generating a 532-nm QPSK data channel. Lenses are used to produce an output collimated beam ~3 mm in diameter. The power of the transmitted signal at 532 nm is controlled to be ~10 dBm. Subsequently, the generated data beam is transmitted through a 0.6-m water tank. The scattering effect is emulated by a diluted commercial antacid solution (Maalox®) [18]. Different concentration of the Maalox® solution results in different scattering strengths of the water channel. At the Rx, the 532-nm data channel is coupled through a collimator into a single-mode fiber (SMF), combined with the ~532-nm LO from a separate ~1064-nm laser source, and mixed with the LO at an amplified free-space coupled photodiode (FS-PD) for the coherent heterodyne detection. The power of the LO is fixed to be ~-1.5 dBm. The SMF with collimator has a narrow field of view. As a result, only the ballistic light is captured by the Rx, which reduces some scattering-induced effects, e.g., the time-spreading of the signal [19]. Based on Beer's law, we characterize the scattering strengths by measuring the on-axis power loss in fiber compared with the clearwater case [18]. We tune the wavelength of the ~1064-nm LO laser to adjust the frequency offset Δf between signal and LO at ~532 nm. Δf is kept being ~1.5 times the channel bandwidth (B), producing a guard band to avoid signal-signal beating interference (SSBI) during heterodyne detection. To compare scattering-induced degradations to coherent detection and IM/DD system, we change the phase modulator to an intensity modulator. PAM4 and on-off keying (OOK) data signals are generated and transmitted through the same scattering strength as the QPSK data. Transmitted power is kept the same across all schemes, and LO is turned off for IM/DD configuration.

3. Experimental results

Figure 3 (a) shows the phase-doubling process of the signal during the SHG in the PPLN. The 1064-nm signal is modulated with the first 4 phase levels of an 8-PSK format, i.e., $\pi/8$, $3\pi/8$, $5\pi/8$, and $7\pi/8$. After going through the PPLN, the phase is doubled to $\pi/4$, $3\pi/4$, $5\pi/4$, and $7\pi/4$, respectively, corresponding to the 4 phase levels of the QPSK signal at 532 nm. To obtain a high-quality QPSK signal, the phase division should be carefully adjusted by tuning the driving voltage fed to the phase modulator. Fig. 3 (b) shows the experimentally measured back-to-back 8-Gbit/s data constellations and error vector magnitudes (EVMs) at 1064 and 532 nm with 3 different phase divisions. The results at 1064 nm are measured using heterodyne detection with the two lasers without going through the PPLN. As shown in Fig. 3 (b1), when the initial signal has a proper phase division, an EVM of 13.8% and 16.1% is achieved before and after the SHG. However, if the phase division modulated at 1064 nm is either smaller or larger than the proper one, as shown in Fig. 3 (b2), the phase level converted to 532 nm deviates from the ideal QPSK format. As a result, the signal quality worsens with an EVM of >~38% for the QPSK signal. It should be noted that the EVM is calculated based on standard 8-PSK and QPSK constellation points for 1064 and 532 nm, respectively. It is worth mentioning that the driving voltage to the phase modulator for a proper phase division is determined by the Vπ of the phase modulator, which is changed with different data rates.

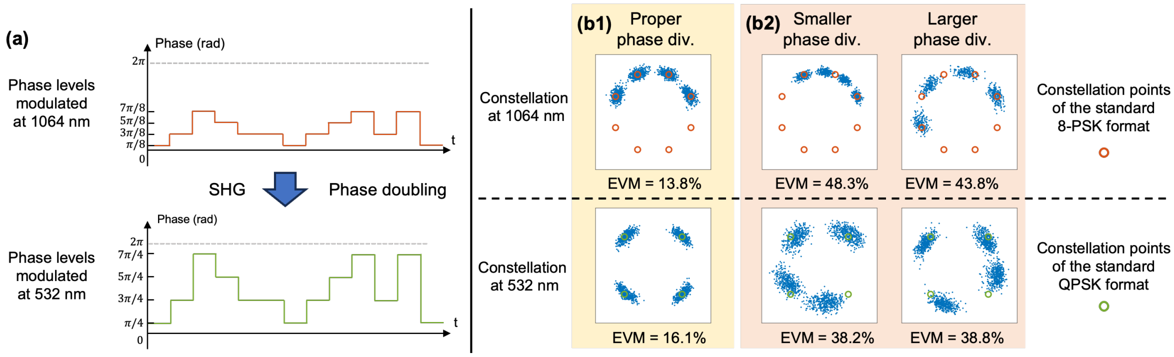

Fig. 3 (a) The concept of the phase doubling process of the signal during SHG in the PPLN. Measured 8-Gbit/s data constellations and EVMs at 1064 and 532 nm with (b1) proper, and (b2) smaller or larger phase divisions. The phase division of the signal is proportional to the driving voltage to the phase modulator. The EVMs are calculated based on standard 8-PSK and QPSK constellation points for 1064 and 532 nm, respectively.

Figure 4 (a) shows the data constellations and corresponding EVMs for 2- and 8-Gbit/s QPSK data channels under clearwater. We observe some phase noise/distortions from the resulting data constellations. This might be due to (i) the laser linewidth of the signal and LO lasers (~500-kHz linewidth), and (ii) the limited bandwidth of our phase modulator. As shown in Fig. 4 (b), we measure the BER performance of 2- and 8-Gbit/s QPSK signals under different scattering strengths. The results show that the BER can reach below the 20% soft-decision forward correction (SD-FEC) limit under scattering with γL up to 8.2 and 6.5 for 2- and 8-Gbit/s QPSK data channels, respectively. The corresponding minimum receiving optical power is -37.8 dBm and -29.8 dBm (system loss ~11.8 dB). Fig. 4 (c1-c4) shows the pictures of the water tank during the experiment with clearwater, and 3 examples of scattering strengths that correspond to the 3 insets in Fig. 4 (b). Fig. 4 (d) compares the performance of the coherent detection and IM/DD link through scattering. To compare the degradation induced by underwater scattering, we control the transmitted power to be the same (~10 dBm) for both schemes and turn off the LO when testing the IM/DD scheme. As shown in Fig. 4 (d), the 2-Gbit/s QPSK, OOK, and PAM4 signals could all be recovered with an EVM of <~13% in clearwater. Under scattering with γL of 6.4, the 2-Gbit/s OOK and PAM4 signal cannot be recovered due to the optical power reaching the Rx lower to its sensitivity. However, the 2-Gbit/s QPSK data is more resilient to the scattering-induced loss, and the signal could still be recovered with an EVM of 21.5%.

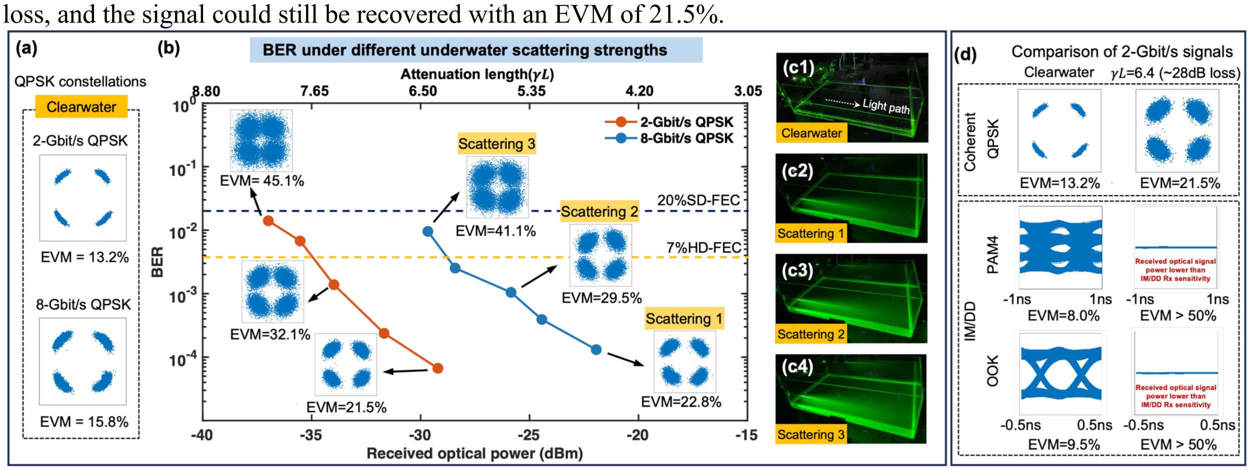

Fig. 4 (a) Data constellation and EVM for 2- and 8-Gbit/s QPSK data channels under clearwater. (b) BER performance of the QPSK data channel under different scattering strengths. Insets show constellations and EVMs of 6 examples of scattering strengths. The picture of the water tank with (c1) clearwater, and (c2-c4) 3 examples of scattering strengths. (d) Data constellations/eye diagrams and EVMs of the 2-Gbit/s signal with phase modulation & coherent detection and IM/DD in clearwater and under a γL of 6.4. The signal is normalized based on the clearwater case when plotting the eye diagrams of the IM/DD system.

Acknowledgment: ONR through MURI Award N00014-20-1-2558; Airbus Institute for Engineering Research; Air Force Office of Scientific Research (sub-award of FA9453-20-2-0001).

Reference: **[1]** F. Hanson al., Appl. Opt., 47, 277 (2008). **[2]** H. Kaushal et al., IEEE Access, 4, 1518 (2016). **[3]** X. Sun et al., J. Light. Technol., 38, 421 (2020). **[4]** S. Zhu et al., Prog. Quantum. Electron., 73, 100274 (2020). **[5]** M. F. Ali et al., IEEE Access, 10, 22169 (2022). **[6]** C. Shen et al., Opt. Express, 24, 25502 (2016). **[7]** J. Wang et al., Opt. Express, 27, 12171 (2019). **[8]** W. S. Tsai et al., Sci. Rep., 9, 8605 (2019). **[9]** Y. Ren et al., Sci. Rep., 6, 33306 (2016). **[10]** K. Kikuchi, J. Light. Technol., 34, 157 (2016). **[11]** K. Morgan et al., IEEE Int. Conf. Commun. Workshops (2020). **[12]** G. N. Arvanitakis, IEEE Photon. J., 12, 7901210 (2020). **[13]** E. Robertson et al., J. Light. Technol., 41, 5209 (2023). **[14]** Y. Wang et al., Opt. Express, 31, 32516 (2023). **[15]** B. Cochenour, et al., OCEANS 2007, Vancouver (2007). **[16]** X. Tang et al., Opt. Express, 29, 19340 (2021). **[17]** X. Zeng et al., Opt. Lett., 47, 222 (2022). **[18]** B. Cochenour et al., Opt. Lett. 35, 2088 (2010). **[19]** B. Cochenour et al., IEEE J. Ocean. Eng. 38, 730 (2013).